

Adaptive Traveling Wave-Based Algorithm for Time Alignment of Transmission Line Fault Records

Felipe V. Lopes, Tiago R. Honorato, Gustavo A. Cunha, Nilo S. S. Ribeiro,
Paulo Lima, Andrei Coelho, Daniel Becker

Abstract—In this paper, an adaptive traveling wave (TW)-based algorithm for time alignment of transmission line fault records is presented. The solution analyzes only the arrival times of incident and fault-reflected TWs at both line terminals, adapting itself to the line travel time. As a result, it overcomes the need for line travel time settings, as required by earlier TW-based time synchronization approaches, leading the proposed method to be more robust to line parameters uncertainties. To evaluate the proposed algorithm, simulated and real fault records are assessed, considering different time alignment error levels. The results demonstrate that the proposed approach is reliable and able to synchronize local and remote line fault records with accuracy of few microseconds.

Keywords—Fault records, fault-induced transients, time synchronization, transmission lines, traveling waves.

I. INTRODUCTION

ANALYZING two-terminal transmission line fault records is a crucial task that supports various post-event studies, such as: fault diagnosis, protection schemes assessment and sequence-of-event analysis [1]. In these procedures, the alignment of fault records is of utmost importance to evaluate local and remote data under the same time reference. Hence, time synchronization means have been widely discussed in the literature since the early stages of multi-terminal transmission networks applications [2]–[4].

The Global Positioning System (GPS) has been widely applied to synchronize signal sampling and time-stamping processes in line monitoring devices [1], [2]. As an alternative for time synchronization in specific lines, communication channel-based techniques have been also used, such as the ping-pong method, which often requires channel latency to present symmetry and low variability to properly compensate time displacements between local and remote data [5],

[6]. However, when the GPS signal is lost or if the communication channel does not meet the requirements for time synchronization procedures, local and remote signals may be recorded asynchronously, jeopardizing two-terminal data post-fault studies [7], [8]. Thus, utilities worldwide have demonstrated great interest in practical time alignment methodologies capable of providing particular time references for both phasor- and time-domain-based applications, which gain further importance when GPS and communication channels are out-of-service.

In the literature, several works reporting time alignment algorithms for phasor-based applications can be found [9]–[12]. These techniques usually consider two-terminal line phasor measurements to calculate synchronization terms that compensate fundamental component phase angle errors in line unsynchronized terminals in relation to an adopted reference bus. However, although these solutions are promising for phasor-based applications, they are affected by distortions in the fundamental component phasors (such as those caused by instrument transformers transients, frequency deviations, DC decaying component, among others [8]), in such a way that their accuracy may not be suitable for time-domain studies within narrow time windows.

Aiming to improve the accuracy of the above-mentioned time alignment procedures when neither GPS nor communication channels are available, TW-based time synchronization methods have been proposed [7], [8]. Aerial and ground mode TWs are analyzed in [7], and different time alignment formulations are presented for grounded and ungrounded faults. On the other hand, to overcome problems due to the high attenuation of ground mode TWs, in [8], a method that requires only the analysis of aerial mode TWs is presented, and an automated synchronization scheme for field applications is proposed. In both mentioned approaches, a time synchronization term κ is calculated considering a given local terminal as reference and, then, κ is added to the remote bus timestamps to align the records time references.

Although the techniques presented in [7] and [8] have shown to be accurate, they require the line travel time τ to be set. In practical situations, τ can present uncertainties when it is calculated by means of cataloged line electrical data, mainly because these parameters are usually computed only at the fundamental frequency. Hence, line energization tests are usually recommended to be carried out whenever the τ setting is required. Even so, if line energization tests are not possible, rough τ values are often used, what can jeopardize the performance of the time synchronization approaches reported

Felipe V. Lopes is with the Department of Electrical Engineering at Federal University of Paraíba (UFPB), 58051-900, Campus I, João Pessoa-PB, Brazil. (e-mail: felipelopes@cear.ufpb.br).

Tiago R. Honorato, and Gustavo A. Cunha are with the Department of Electrical Engineering at University of Brasília (UnB), 70910-900 Brasília-DF, Brazil. (e-mail: tiagohonorato@lapse.unb.br, gustavocunha@lapse.unb.br).

Nilo S. S. Ribeiro is with Eletronorte, Brasília, Brazil (e-mail: nilo@eletronorte.com.br).

Paulo Lima is with Schweitzer Engineering Laboratories, Inc., Campinas 13069-320, Brazil (e-mail: paulo_lima@selinc.com).

Andrei Coelho is an independent electrical engineering, Campinas 13087-500, Brazil (e-mail: andrei_fc@hotmail.com).

Daniel Becker is with Cia Estadual de Ger. e Transm. de Energia Elétrica (CEEE-GT), Rio Grande do Sul, Brazil (e-mail: danielb@ceee.com.br).

in [7] and [8]. Moreover, even if the energization test is carried out, from the testing maneuver instant until the fault inception on the line (which is a period that may range from few instants to several months), weather and system operating conditions can change, so that τ can present unpredictable variations.

From the above-mentioned context, it is noticed that making existing time alignment techniques adaptive to uncertainties in τ is a practical way to enhance the procedures proposed in [7] and [8]. Thus, in this work, an adaptive TW-based solution for two-terminal fault records time alignment is proposed, which analyzes the arrival times of incident and fault-reflected TWs at both line ends, canceling τ from the κ calculation formulas. As a result, the algorithm becomes adaptive to uncertainties in line parameters, leading κ to be more robust and reliable for real world applications.

To validate the proposed algorithm, simulated and real TW fault records are assessed, considering different levels of local and remote data synchronization errors. Also, two practical methodologies to apply the proposed algorithm are presented, allowing the users to calculate κ from data promptly provided by commercially available TW-based line monitoring devices. The obtained results show that the proposed algorithm is reliable, easy-to-apply and able to accurately align local and remote records. The obtained results show that the proposed solution can reach a time synchronization accuracy of few microseconds, which is comparable to those verified when GPS or communication channel-based solutions are applied.

II. PROPOSED TIME ALIGNMENT ALGORITHM

The proposed algorithm is an enhanced version of the one reported in [8]. It includes practical procedures to facilitate the calculation of the time synchronization term κ in real systems when single-ended phasor- and TW-based fault location functions are available, which are referred here as **SEZFL** and **SETWFL**, respectively. Basically, the goal is to calculate κ taking a given local line terminal as reference, and then, to add κ to the opposite unsynchronized remote line end where the time reference must be corrected.

In order to explain the proposed algorithm, Fig. 1 is shown. It depicts the Bewley diagram of aerial mode TWs in a given line that connects two buses, called Bus L (local) and Bus R (remote). TW recorders are assumed to be installed at both line ends, which can be or not equipped with SETWFL functions, such as verified in existing TW devices [13], [14]. The index ‘1’ stands for aerial mode quantities, being: t_0 the fault inception instant, t_{ref} the reference time, d the fault distance from Bus L, ℓ the line length, t_{L1} , t_{R1} , t_{L1r} and t_{R1r} the real arrival times of the first incident aerial mode TWs and fault-reflected TWs at buses L and R, respectively, t_{R1}^* and t_{R1r}^* the measured arrival times of the first incident and fault-reflected aerial mode TWs at Bus R, respectively, and ξ the Bus R time error in relation to the Bus L time reference t_{ref} . It can be also seen that measured TW patterns are not consistent with the expected real ones when the local terminal is taken as reference, revealing that a time alignment error exists in Bus R records.

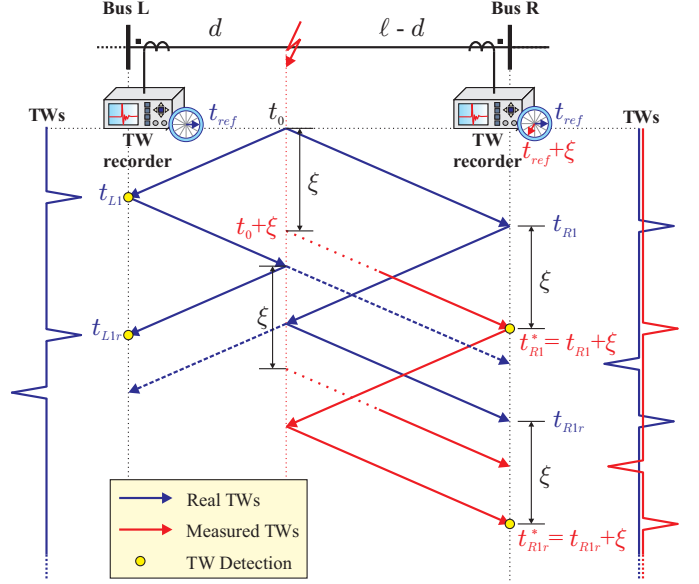


Fig. 1. Bewley diagram considering an internal fault on a two-terminal transmission line.

A. Fundamentals on κ Calculation

In the proposed algorithm, κ is computed by combining both classical single- and double-ended TW-based fault location methods, in which the fault distance d is calculated respectively by:

$$d = (t_{L1r} - t_{L1}) \cdot (\ell/2\tau), \quad (1)$$

$$d = \{\tau - [(t_{R1}^* + \kappa) - t_{L1}]\} \cdot (\ell/2\tau), \quad (2)$$

where τ is the line travel time and t_{R1}^* is the instant t_{R1} time displaced by ξ , as shown in Fig. 1. Thus, according to [8], (1) and (2) return the same fault distance estimations uniquely if $\kappa = -\xi$, so that κ is given by:

$$\kappa = \tau - (t_{R1}^* - t_{L1}) - (t_{L1r} - t_{L1}). \quad (3)$$

In practice, detecting t_{L1} and t_{R1}^* is relatively easy if high energy TWs are launched from the fault [1]. Also, real TW-based line monitoring devices have been released with functionalities that detect t_{L1r} [20], which greatly simplifies the application of (3). Thus, assuming τ as an user-defined setting consists in the most critical issue for (3), mainly if τ is roughly estimated without performing transmission line energization tests.

B. Enhancing κ Calculation

In order to make the proposed algorithm adaptive in relation to τ uncertainties, this setting is estimated by analyzing fault-induced transients themselves. As a result, line energization maneuvers to obtain τ are no longer required, and κ becomes more robust to deviations in line parameters. To do so, consider the application of (1) at the Bus R shown in Fig. 1. By doing so, the distance $\ell - d$ can be calculated (irrespective of the time displacement ξ value) using:

$$\ell - d = (t_{R1r}^* - t_{R1}^*) \cdot (\ell/2\tau). \quad (4)$$

Adding (1) and (4), and solving for τ , one can obtain that:

$$\tau = 0.5 \cdot [(t_{L1r} - t_{L1}) + (t_{R1r}^* - t_{R1}^*)] . \quad (5)$$

Therefore, substituting (5) in (3), an adaptive formula for κ calculation is obtained as follows:

$$\kappa = 0.5 \cdot [(t_{R1r}^* - t_{R1}^*) - (t_{L1r} - t_{L1})] - (t_{R1}^* - t_{L1}) . \quad (6)$$

Once κ is estimated, remote fault records timestamps can be corrected. As reported in [8], such an alignment can be carried out by editing remote COMTRADE files, simply by adding κ to the fault record initial and trigger instants available in the .cfg file, as well as to TW detection instants, if they are available in .hdr files. This procedure can be manual or automated, but the upload of κ in the Supervisory Control and Data Acquisition (SCADA) is suggested [8], so that it can be used for records synchronization whenever it is required.

III. PRACTICAL APPLICATION OF THE PROPOSED TIME ALIGNMENT ALGORITHM

As shown in (6), κ calculation depends only on the detection of t_{L1} , t_{R1}^* , t_{L1r} and t_{R1r}^* , i.e., τ is no longer required to be set. The instants t_{L1} and t_{R1}^* are typically estimated by commercially available TW-based line monitoring devices [13], [14], [16]. Furthermore, besides the techniques available in the literature to identify t_{L1r} and t_{R1r}^* [15], [17]–[20], TW devices equipped with fault-reflected TW detection functions are already commercially available for practical applications, such as those described in [13] and [16], which apply the approach proposed in [20].

Despite the existing solutions to detect t_{L1} , t_{R1}^* , t_{L1r} and t_{R1r}^* , these time instants are usually dedicated to **TW-based fault location** and high-speed protection functionalities, so that their values are not always explicitly informed in fault records. Depending on the used devices, t_{L1} and t_{R1}^* can be found in .hdr files, but t_{L1r} and t_{R1r}^* are often omitted, being only available for internal SETWFL functions. Therefore, if SETWFL method outputs are available (or even the phasor-based SEZFL results), fault distance estimations can be used to support the detection of t_{L1r} and t_{R1r}^* , provided that high sampling rates are available. Based on that, in the next sections, two different methodologies are presented for κ calculation. In both, only current TWs are analyzed, since the frequency response of current transformers is better than those of capacitive voltage transformers, which are typically applied in transmission networks [1].

A. Methodology M1: SETWFL Function Unavailable

In the application methodology M1, it is assumed that SETWFL schemes are not available and that only SEZFL estimations can be accessed in line monitoring devices. Hence, t_{L1} , t_{R1}^* , t_{L1r} and t_{R1r}^* must be estimated by manual inspection of TW fault records. The detection of the first incident TWs can be carried out just by verifying the time instant at which the first fault-induced transients occur in the evaluated signals, but the manual identification of t_{L1r} and t_{R1r}^* require further procedures, as described next.

Aiming to simplify the proposed algorithm application, (6) is rearranged to become a function of the time periods $\Delta T_{RrLr} = (t_{R1r}^* - t_{L1r})$ and $\Delta T_{RL} = (t_{R1}^* - t_{L1})$, yielding:

$$\kappa = 0.5\Delta T_{RrLr} - 1.5\Delta T_{RL} . \quad (7)$$

A practical procedure to identify fault-reflected TWs is to use SEZFL estimations $d_{z,L}$ (fault distance from Bus L) and $d_{z,R}$ (fault distance from Bus R) as auxiliary variables to create search windows ΔT_{search} over the time, within which the TWs of interest must be sought [21]. Even when SEZFL estimations from only one terminal exists, the complementary distance from the other line end can be used to calculate ΔT_{search} , requiring the knowledge of the line length ℓ (i.e., if $d_{z,L}$ is available, $d_{z,R} = \ell - d_{z,L}$ can be assumed, if necessary) and rough values of τ (as commonly available in TW-based applications, despite possible uncertainties). Thus, one can estimate time instants $t_{rb,L}$ and $t_{rb,R}$ at which TWs reflected back from the fault point are expected to show up in the evaluated local and remote TW records, respectively, which are given by:

$$t_{rb,L} = t_{L1} + \frac{2\tau(d_{z,L})}{\ell} , \quad (8)$$

$$t_{rb,R} = t_{R1}^* + \frac{2\tau(d_{z,R})}{\ell} , \quad (9)$$

being the search field ΔT_{search} defined as follows:

$$\Delta T_{search,bus} = [t_{rb,bus} - M ; t_{rb,bus} + M] , \quad (10)$$

where *bus* stands for buses L or R, $\Delta T_{search,bus}$ is the fault-reflected TW search window at terminal *bus*, and M is the search window margin, taken in this paper as 30 μ s.

Even using the search windows ΔT_{search} , for the sake of reliability, a polarity analysis of fault-reflected TWs is recommended. To do so, it must be firstly understood that substations in transmission networks traditionally present several line bays, and in the case of high frequency transients (as those caused by TW propagation), spurious capacitances take place along the local and remote busbars. Furthermore, at the fault point, the TWs see an equivalent impedance formed by the fault resistance in parallel to the line surge impedance, which is usually smaller than the line surge impedance from where the TWs propagate [15]. As a result, the line terminals and the fault point commonly consist in discontinuities with positive reflection coefficients for current TWs. Thereby, no polarity inversion is expected to be observed between the first incident TWs and those reflected back from the fault point, and this condition can be taken into account during the analysis of ΔT_{search} content, improving the t_{L1r} and t_{R1r}^* detection.

B. Methodology M2: SETWFL Function Available

In the time alignment methodology M2, it is assumed that SETWFL estimations from buses L and R are available, which will be called hereafter $d_{TW,L}$ and $d_{TW,R}$, respectively. To facilitate the description of this methodology, (6) is rewritten as a function of the time periods $\Delta T_{Lr} = (t_{L1r} - t_{L1})$, $\Delta T_{Rr} = (t_{R1r}^* - t_{R1}^*)$ and $\Delta T_{RL} = (t_{R1}^* - t_{L1})$, so that:

$$\kappa = 0.5(\Delta T_{Rr} - \Delta T_{Lr}) - \Delta T_{RL} . \quad (11)$$

From (1) and (4), in practice, considering that τ is set in TW-based devices with a given value τ_{set} , and assuming that $d_{TW,L}$ and $d_{TW,R}$ have been computed, it can be derived that $\Delta T_{Lr} = \frac{2\tau_{set}d_{TW,L}}{\ell}$ and $\Delta T_{Rr} = \frac{2\tau_{set}d_{TW,R}}{\ell}$. Thereby, substituting these relations in (11) results in:

$$\kappa = (d_{TW,R} - d_{TW,L}) \cdot (\tau_{set}/\ell) - \Delta T_{RL} . \quad (12)$$

In this case, time instants t_{L1} and t_{R1}^* are used to calculate ΔT_{RL} , and they must be identified by manual inspection of fault records. Even so, the application of $d_{TW,L}$ and $d_{TW,R}$ directly in κ calculation greatly simplifies the time alignment process. It should be noticed that, in practice, SETWFL estimations can be available at only one line end. Hence, as SETWFL are expected to be highly accurate, if only $d_{TW,L}$ is available, $d_{TW,R} \approx \ell - d_{TW,L}$ can be assumed, and thus, (11) becomes:

$$\kappa = [(\ell - 2d_{TW,L}) \cdot (\tau_{set}/\ell)] - \Delta T_{RL} , \quad (13)$$

otherwise, if only $d_{TW,R}$ is available, Bus R must be taken as the reference terminal, and (13) can be used as well.

It is worthy to emphasize that, in this methodology, although τ_{set} is used in (12) and (13), it does not affect the accuracy of κ . The only requirement in this case is that τ_{set} has been used to compute $d_{TW,L}$ and/or $d_{TW,R}$. By doing so, uncertainties in the real τ value are canceled, maintaining the proposed algorithm adaptive to line parameter variations.

IV. CASE STUDIES

In order to evaluate the proposed time alignment algorithm, laboratory tests considering simulated and real TW records are carried out. Initially, two-terminal line fault records are generated in synchronism, and then, ξ errors are added to remote terminal data. This procedure is taken into account to quantify the final time synchronization error E_s , which is given by $E_s = |\xi + \kappa|$. However, some analyzed real records are related to scenarios in which local and remote devices indeed present time synchronization problems and, thus, as ξ is not known a priori, in these cases, the results are validated by inspecting Bewley diagrams.

A. Simulated Scenarios

The Alternative Transients Program (ATP) is used to generate records of faults on a 230 kV/60 Hz line, 344.16 km long, with $\tau = 1155.1388 \mu\text{s}$, which represents in detail a power network in operation in Brazil, such as reported in [8]. Figs. 2 and 3 present the system topology and transmission line data (tower geometry, conductor information and ground resistivity), respectively, but further details on the system are omitted due to confidentiality reasons. The frequency dependent Jmarti line model is taken into account and terminal substations are modeled in detail, such as reported in [8]. After each analyzed case, simulated records are played back into real TW-based line monitoring devices, which are equipped with a SETWFL function and A/D converters with sampling rates equal to 1 MHz [13]. Therefore, the ATP time step was set to 1 μs , allowing playback tests internally in the TW recorders memory [13], guaranteeing proper transients representation.

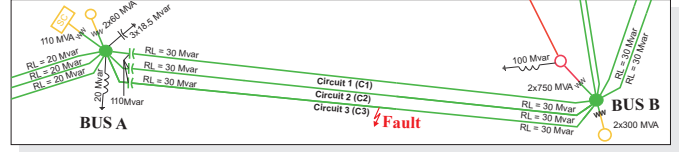


Fig. 2. Evaluated 230 kV/60 Hz power system.

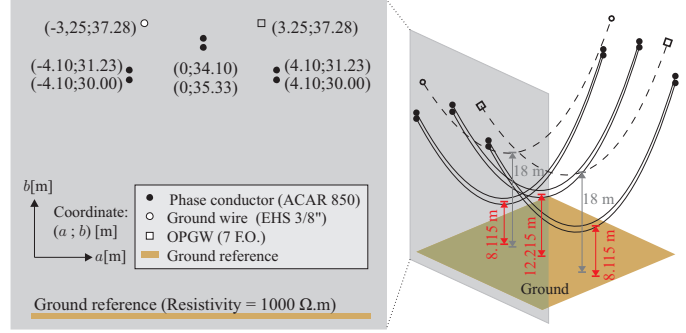


Fig. 3. Simulated transmission line data [8].

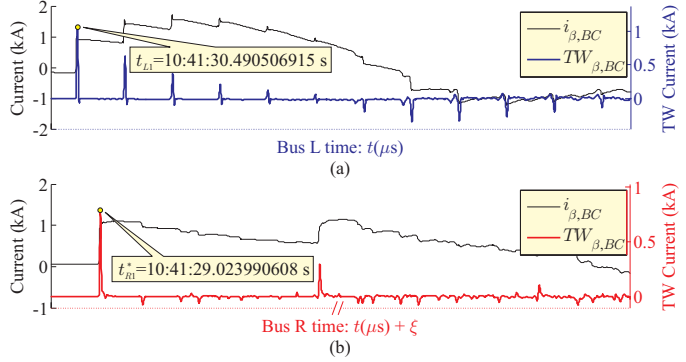


Fig. 4. Simulated case S1 records taken from: (a) Bus B; (b) Bus A.

Fig. 4 illustrates the two-terminal records obtained from an ATP simulation called case S1. It consists in a BC solid fault, $d = 50.59$ km far from Bus B, and initiated at the BC line voltage peak, with $\xi = -1.467328$ s at Bus A. Hence, the Clarke's component $i_{\beta,BC}$ is analyzed, as recommended in [22] and, since the used TW devices apply digital filters to extract TW information, original current signals are available, so that the modal quantity is calculated and illustrated in conjunction with its filtered version $TW_{\beta,BC}$ in Fig. 4.

In this case, $d_{TW,L} = 51.133$ km and $d_{TW,R} = 292.892$ km are obtained from the TW-based devices, so that κ is computed by means of the methodology M2. Moreover, regarding the first incident TWs, $\Delta T_{RL} = -1.466516307$ s is obtained. Thus, being $\tau_{set} = \tau$, from (12), it is obtained that:

$$\begin{aligned} \kappa &= (292.892 - 51.133) \cdot \frac{1155.1388\mu}{344.16} - (-1.466516307) \\ &= 1.467327747 \text{ s} , \end{aligned} \quad (14)$$

which means that local and remote records were synchronized with accuracy equal to $E_s = |\xi + \kappa| = 0.253 \mu\text{s}$.

It should be pointed out that, if τ_{set} is erroneously set, while ΔT_{RL} is not affected, $d_{TW,L}$ and $d_{TW,R}$ can present errors. To

exemplify this situation, the erroneous setting $\tau_{set} = 1000 \mu\text{s}$ is considered, yielding $d_{TW,L} = 59.066 \text{ km}$ and $d_{TW,R} = 338.309 \text{ km}$. Although these estimations present fault location errors of about 8.476 km and 44.738 km, respectively, the result shown in (14) is not affected, attesting that the proposed algorithm is indeed robust to line parameter uncertainties.

To further evaluate the proposed algorithm, three additional simulated cases (S2, S3 and S4) are studied, varying ξ , fault distance d , fault resistance R_f , fault type, and fault inception angle θ (under a sinusoidal reference). Table I presents the description of each case and the obtained results. In all studied scenarios, errors E_s did not exceed the order of $1 \mu\text{s}$, which are comparable to those verified when GPS and communication channel-based time synchronization solutions are used¹.

TABLE I
SIMULATED CASES.

Variable	Case S2	Case S3	Case S4
Fault Type	BCG	AG	AG
d	77.78 km	123.90 km	55.07 km
R_f	30 Ω	Solid fault	30 Ω
θ	90°	50°	90°
ξ (s)	+4.000000000	+7.0000030046	+1.0000003600
κ (s)	-3.9999996124	-7.0000028234	-0.9999994272
E_s (μs)	0.3876	0.181	0.9328

B. Real World Scenarios

1) *Case R1 - CG, $\ell = 28.40 \text{ km}$, $d = 16.790 \text{ km}$:* In this case, fault records are originally synchronized and, therefore, $\xi = +1.12516 \text{ s}$ is added to remote timestamps. In this system, $\tau = 99.88 \mu\text{s}$ is set in TW devices and, although they are equipped with SETWFL functions at both line ends, only $d_{TW,L} = 16.394 \text{ km}$ is available, so that (13) is applied. In this scenario, the TW devices are the same used in the previous case S1, being the sensitized modal current and TW digital filter outputs presented in Fig. 5. From the record inspection, $\Delta T_{RL} = 1.125142208 \text{ s}$. Hence, being $\tau_{set} = \tau$, one obtains:

$$\begin{aligned} \kappa &= (28.40 - 2 \cdot 16.394) \cdot \frac{99.88 \mu}{28.40} - 1.125142208 \\ &= -1.125157640 \text{ s}, \end{aligned} \quad (15)$$

i.e., $E_s = |\xi + \kappa| = 2.359 \mu\text{s}$ is verified.

2) *Case R2 - CG, $\ell = 122.03 \text{ km}$, $d = 99.58 \text{ km}$:* In this case, $\xi = +2.320 \text{ s}$ in the remote time reference is emulated. In the analyzed system, $\tau = 414.99966 \mu\text{s}$, and the TW devices are not equipped with SETWFL functions. Thereby, the methodology M1 is used to compute κ , using (7). To do so, the SEZFL estimation from the reference Bus L $d_{z,L} = 101.909 \text{ km}$ is considered to apply (8) and then (9), assuming $\tau_{set} = \tau$ and $d_{z,R} = \ell - d_{z,L}$. It is worthy to mention that the records evaluated from this case onwards are taken from devices that apply analog band-pass filters to

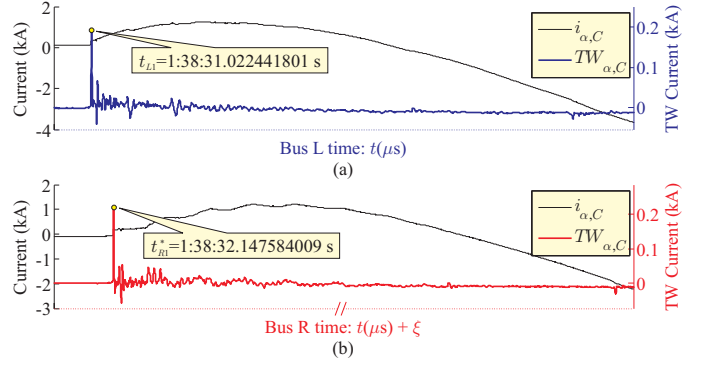


Fig. 5. Case R1 records: (a) Reference bus; (b) Unsynchronized bus.

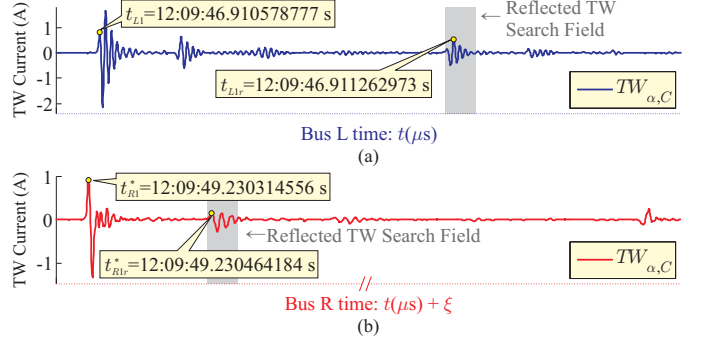


Fig. 6. Case R2 records: (a) Reference bus; (b) Unsynchronized bus.

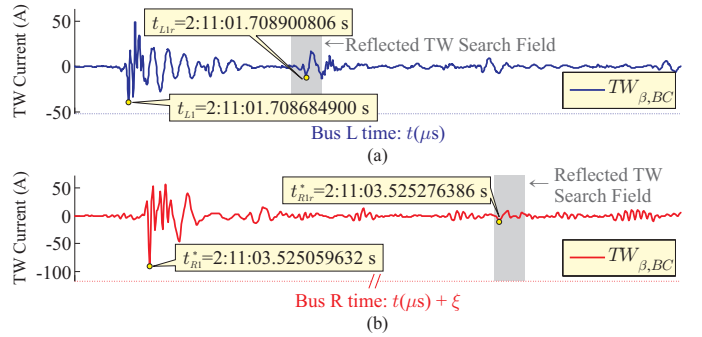


Fig. 7. Case R3 records: (a) Reference bus; (b) Unsynchronized bus.

extract TW information [14]. Thus, the original current signals are not available, so that only the filtered signals are presented. Fig. 6 shows the sensitized modal TWs and the estimated search fields. In this scenario, $\Delta T_{RrLr} = 2.319201211 \text{ s}$ and $\Delta T_{RL} = 2.319735779 \text{ s}$ are obtained, so that:

$$\begin{aligned} \kappa &= 0.5 \cdot 2.319201211 - 1.5 \cdot 2.319735779 \\ &= -2.320003063 \text{ s}, \end{aligned} \quad (16)$$

i.e., $E_s = |\xi + \kappa| = 3.063 \mu\text{s}$ is obtained.

3) *Case R3 - BCG, $\ell = 65.20 \text{ km}$, $d = 32.26 \text{ km}$:* In this case, $\xi = +1.816372 \text{ s}$ is simulated, $\tau = 220.7957 \mu\text{s}$, and SETWFL functions are not available, i.e., (7) is used. From the local SEZFL function, $d_{z,L} = 30.933 \text{ km}$. Hence, using $\tau_{set} = \tau$ and assuming $d_{z,R} = \ell - d_{z,L}$, the reflected TWs search fields are estimated, as depicted in Fig. 7.

¹From the authors experience, synchronization errors of up to $10 \mu\text{s}$ would be acceptable for post-event records analysis in microsecond time scale.

From the records evaluation, $\Delta T_{RrLr} = 1.81637558$ s and $\Delta T_{RL} = 1.816374732$ s are obtained, in such a way that:

$$\begin{aligned} \kappa &= 0.5 \cdot 1.81637558 - 1.5 \cdot 1.816374732 \\ &= -1.816374308 \text{ s}, \end{aligned} \quad (17)$$

i.e., $E_s = |\xi + \kappa| = 2.308 \mu\text{s}$.

4) *Case R4 - AG, $\ell = 101.930$ km, d information unavailable:* In this scenario, an AG fault occurs on a transmission line 101.930 km long, with $\tau = 341.305669894 \mu\text{s}$. The fault point was not identified in the field by line inspection crews and SETWFL functions are not available. On the other hand, SEZFL function at Bus L is enabled, resulting in $d_{z,L} = 25.58$ km. Thus, $d_{z,R} = \ell - d_{z,L}$ and $\tau_{set} = \tau$ are assumed to estimate the fault-reflected TWs search fields at the line ends, and then, κ is estimated using (7). Fig. 8 shows the TW filtered signals and the detected wavefronts arrival instants. From the fault records analysis, it is calculated that $\Delta T_{RrLr} = -13.176327701$ s and $\Delta T_{RL} = -13.176675366$ s, thereby:

$$\begin{aligned} \kappa &= 0.5 \cdot (-13.176327701) - 1.5 \cdot (-13.176675366) \\ &= 13.176849198 \text{ s}. \end{aligned} \quad (18)$$

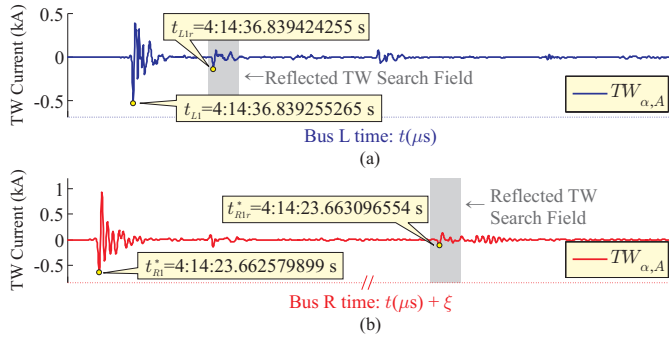


Fig. 8. Case R4 records: (a) Reference bus; (b) Unsynchronized bus.

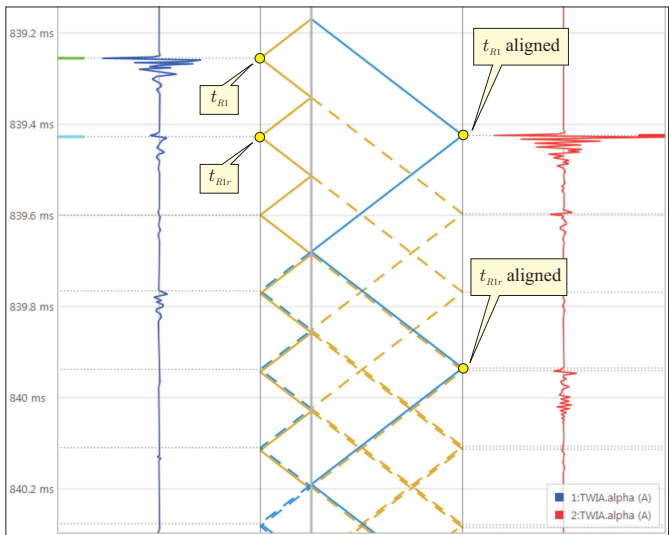


Fig. 9. Case R4 κ validation via Bewley diagram.

Since in this case ξ is not known a priori, Fig. 9 depicts the obtained Bewley diagram built after the proposed algorithm application. It is noticed that, by adding κ to the remote bus time stamps, fault transients are consistent with the Bewley diagram, attesting the validity of the proposed methodology.

5) *Case R5 - CG, $\ell = 127.070$ km, d information unavailable:* This last evaluated real case is presented in Fig. 10. Records related to a CG fault occurred on a transmission line 127.07 km long, with $\tau = 429.374 \mu\text{s}$ are evaluated. The fault distance was not confirmed by the line inspection crews, and the TW devices are not equipped with SETWFL functions, i.e., κ is calculated using (7). In this scenario, $d_{z,L} = 51.49$ km was estimated and, therefore, assuming $d_{z,R} = \ell - d_{z,L}$ and $\tau_{set} = \tau$, it is obtained that $\Delta T_{RrLr} = 21.183996772$ s and $\Delta T_{RL} = 21.183881357$ s. Therefore, κ is given by:

$$\begin{aligned} \kappa &= 0.5 \cdot 21.183996772 - 1.5 \cdot 21.183881357 \\ &= -21.18382365 \text{ s}. \end{aligned} \quad (19)$$

Fig. 11 shows the Bewley diagram obtained after the proposed time alignment procedure. Since fault record transients are all consistent with the Bewley diagram, a successful alignment of local and remote records is attested.

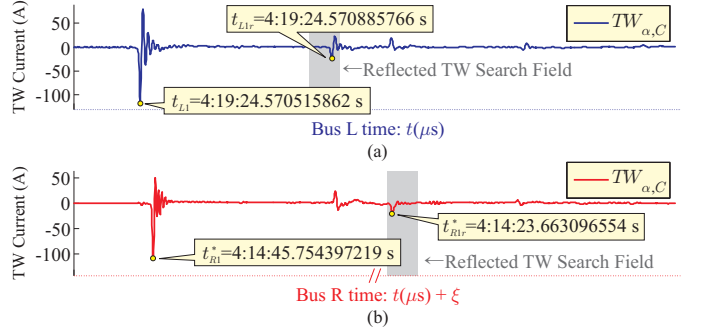


Fig. 10. Case R5 records: (a) Reference bus; (b) Unsynchronized bus.

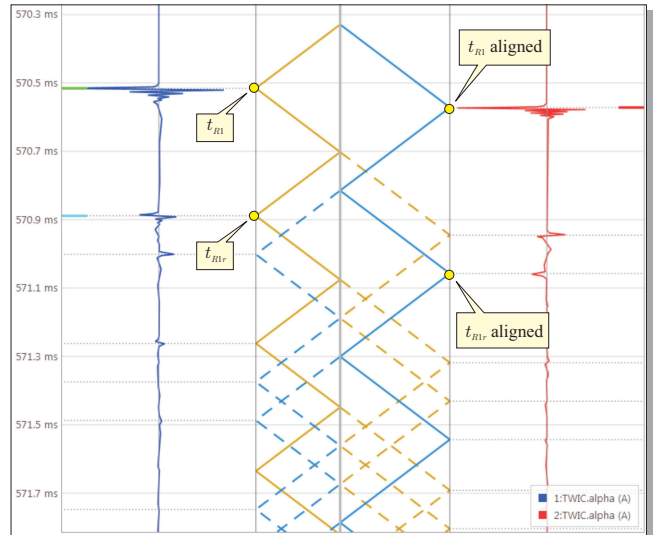


Fig. 11. Case R5 κ validation via Bewley diagram.

V. CONCLUSIONS

In this paper, an adaptive TW-based fault records time alignment algorithm is presented. It calculates a time synchronization term κ , which is adaptive to the transmission line travel time τ . Thereby, the algorithm is robust to uncertainties in line parameters that may arise in real systems, being more reliable than earlier TW-based time synchronization solutions, which require line parameter-based settings.

To evaluate the proposed algorithm, simulated and real world fault records were analyzed, considering different time displacement errors ξ between local and remote data. Moreover, two real scenarios in which TW devices indeed presented time synchronization errors were considered, being the results validated by means of Bewley diagram inspection.

In all assessed scenarios, the proposed algorithm has shown to be capable of synchronizing local and remote fault records with accuracy that range from fractions to few microseconds. In simulated scenarios, the proposed solution resulted in local and remote data time alignment errors that did not exceed 1 μ s. In the best performance case, the time synchronization accuracy reached the order of 0.1 μ s only, demonstrating the validity of the proposed algorithm. In addition, considering the real-world scenarios in which controlled time synchronization errors were analyzed, the time alignment deviations did not exceed the order of 3 μ s. Even in the assessed cases in which time synchronization errors are unknown, the Bewley diagram inspection has also demonstrated the proposed solution reliability for real-world applications. In fact, in these latter cases, both local and remote TW records matched the expected transient patterns after the proposed algorithm application, attesting that the time synchronization procedure was successfully accomplished. Therefore, one can conclude that the proposed algorithm performance is comparable to those verified when GPS or communication channel-based time synchronization solutions are in service, so that it is a good alternative for records alignment procedures when classical sources of common time reference are unavailable.

ACKNOWLEDGMENT

The authors would like to thank the Coordination for the Improvement of Higher Education Personnel (CAPES) and the University of Brasilia (UnB) for the financial support.

REFERENCES

- [1] M. M. Saha, J. Izykowski, and E. Rosolowski, *Fault Location on Power Networks*, ser. Power Systems. London: Ed. Springer, 2010.
- [2] H. Lee and A. M. Mousa, "GPS travelling wave fault locator systems: investigation into the anomalous measurements related to lightning strikes," *IEEE Transactions on Power Delivery*, vol. 11, no. 3, pp. 1214–1223, Jul 1996.
- [3] P. Moore and P. Crossley, "Gps applications in power systems. i. introduction to gps," *Power Engineering Journal*, vol. 13, no. 1, pp. 33–39, 1999.
- [4] P. A. Crossley, H. Guo, and Z. Ma, "Time synchronization for transmission substations using gps and ieeec 1588," *CSEE Journal of Power and Energy Systems*, vol. 2, no. 3, pp. 91–99, 2016.
- [5] H. J. Altuve and E. O. Schweitzer, *Modern Solutions for Protection, Control and Monitoring of Electric Power Systems*. Pullman, USA: Schweitzer Engineering Laboratories, Inc., 2010.

- [6] B. Kasztenny, N. Fischer, K. Fodero, and A. Zvarych, "Communications and data synchronization for line current differential schemes," in *proceedings of the 38th Annual Western Protective Relay Conference*, Spokane, WA, 2011, pp. 1–4.
- [7] F. V. Lopes and E. J. S. Leite, "Traveling wave-based solutions for transmission line two-terminal data time synchronization," *IEEE Transactions on Power Delivery*, vol. 33, no. 6, pp. 3240–3241, 2018.
- [8] F. V. Lopes, T. Honorato, G. Cunha, and N. Ribeiro, "Transmission line records synchronization based on traveling waves analysis," *IEEE Transactions on Power Delivery*, pp. 1–1, 2020.
- [9] J. Izykowski, E. Rosolowski, P. Balcerek, M. Fulczyk, and M. Saha, "Accurate noniterative fault location algorithm utilizing two-end unsynchronized measurements," *IEEE Transactions on Power Delivery*, vol. 25, no. 1, pp. 72–80, Jan. 2010.
- [10] F. Steinhauser, C. Riesch, and M. Rudigier, "Ieee 1588 for time synchronization of devices in the electric power industry," in *2010 IEEE International Symposium on Precision Clock Synchronization for Measurement, Control and Communication*, 2010, pp. 1–6.
- [11] J. Izykowski, E. Rosolowski, P. Balcerek, M. Fulczyk, and M. Saha, "Fault location on double-circuit series-compensated lines using two-end unsynchronized measurements," *Power Delivery, IEEE Transactions on*, vol. 26, no. 4, pp. 2072–2080, oct. 2011.
- [12] M. C. Cruz, M. Almeida, and M. F. Medeiros Júnior, "A state estimation approach for fault location in transmission lines considering data acquisition errors and non-synchronized records," *International Journal of Electrical Power & Energy Systems*, vol. 78, pp. 663–671, 2016.
- [13] *Ultra-High-Speed Transmission Line Relay Traveling-Wave Fault Locator High-Resolution Event Recorder - T400L*, SEL Schweitzer Engineering Laboratories, 2017.
- [14] *Advanced Line Differential Protection, Automation, and Control System*, Schweitzer Engineering Laboratories, 2018. [Online]. Available: <https://selinc.com/products/411L/>
- [15] E. O. Schweitzer, A. Guzmán, M. V. Mynam, V. Skendzic, B. Kasztenny, C. Gallacher, and S. Marx, "Accurate single-end fault location and line-length estimation using traveling waves," in *13th International Conference on Developments in Power System Protection*, March 2016.
- [16] *Ultra-High-Speed Line Relay - T401L*, SEL Schweitzer Engineering Laboratories, 2020.
- [17] P. A. Crossley and P. G. McLaren, "Distance protection based on travelling waves," *IEEE Transactions on Power Apparatus and Systems*, vol. PAS-102, no. 9, pp. 2971–2983, 1983.
- [18] E. H. Shehab-Eldin and P. G. McLaren, "Travelling wave distance protection-problem areas and solutions," *IEEE Transactions on Power Delivery*, vol. 3, no. 3, pp. 894–902, 1988.
- [19] Aoyu Lei, X. Dong, and S. Shi, "A novel method to identify the travelling wave reflected from the fault point or the remote-end bus," in *2015 IEEE Power Energy Society General Meeting*, 2015, pp. 1–5.
- [20] A. Guzmán, B. Kasztenny, Y. Tong, and M. V. Mynam, "Accurate and economical traveling-wave fault locating without communications," in *2018 71st Annual Conference for Protective Relay Engineers (CPRE)*, 2018, pp. 1–18.
- [21] F. V. Lopes, P. Lima, J. P. G. Ribeiro, T. R. Honorato, K. M. Silva, E. J. S. Leite, W. L. A. Neves, and G. Rocha, "Practical methodology for two-terminal traveling wave-based fault location eliminating the need for line parameters and time synchronization," *IEEE Transactions on Power Delivery*, vol. 34, no. 6, pp. 2123–2134, 2019.
- [22] E. O. Schweitzer, A. Guzmán, M. V. Mynam, V. Skendzic, B. Kasztenny, and S. Marx, "Locating faults by the traveling waves they launch," in *50th Annual Minnesota Power Systems Conference*, November 2014.